Tracking the long-term GW phase evolution for HM Cancri-like binaries with LISA

Naoki Seto

Department of Physics, Kyoto University, Kyoto 606-8502, Japan

(Received 6 June 2023; accepted 7 July 2023; published 25 July 2023)

From prolonged x-ray and optical data of the ultracompact binary HM Cancri, two groups recently measured the second derivative of its orbital frequency. The space gravitational wave detector LISA will detect $\sim 10^4$ Galactic binaries, and their second frequency derivatives will be interesting observational targets for LISA. Here, we forecast the gravitational wave signal analysis for HM Cancri, as an ideal reference system for these numerous binaries. We find that, in its nominal operation period $T \sim 4$ yr, LISA is unlikely to realize a sufficient measurement precision for the reported second frequency derivative of this binary. However, because of a strong dependence on the time baseline, the precision will be drastically improved by extending the operation period of LISA or combining it with other missions (e.g., Taiji and TianQin) in a sequential order.

DOI: 10.1103/PhysRevD.108.023019

I. INTRODUCTION

The Laser Interferometer Space Antenna (LISA) has the potential to detect gravitational waves (GWs) from various astrophysical sources such as merging massive black hole binaries, extreme mass ratio inspirals, and Galactic stellar mass binaries [1]. While the event rates of the systems involving massive black holes are highly uncertain, the Galactic binaries are solid observational targets. In fact, a few tens of compact binaries are currently listed as LISA's verification sources and will be detected at sufficient signal-to-noise ratios [1,2]. HM Cancri is an interacting white dwarf (WD) binary and regarded as one of the loudest GW sources in the list.

In this paper, since we focus on GW observation, we basically use the GW frequency f of a binary, not its orbital frequency. For a circular binary such as HM Cancri, the GW frequency is twice the orbital frequency. Correspondingly, if necessary, we will automatically make appropriate conversions for the reported values in the literature (often given for the orbital frequency). The GW frequency of HM Cancri is $f = 6.2$ mHz, which is the highest frequency in the list [1,2].

Using electromagnetic (EM) data accumulated for HM Cancri in the past $\sim$20 yr, two groups recently measured the acceleration rate of its frequency $\ddot{f}$, for the first time to our knowledge among the verification binaries [3,4]. The second derivative $\ddot{f}$ is expected to contain interesting information on the evolution of the binary (e.g., mass transfer [3–7]; see also [8] for $\dot{f}$) and its environment (e.g., tertiary gravitational perturbation [9,10]).

Owing to its omnidirectional sensitivity, LISA will detect $\sim 10^4$ Galactic binaries, including more than $\sim 10^2$ subsets at $f \gtrsim 6$ mHz [1,11–13]. The obtained results $\ddot{f}$ for HM Cancri will serve as ideal reference values when discussing GW signal analysis for these numerous binaries. In this paper, we study such an observational prospect, paying special attention to HM Cancri. Relatedly, we assort useful analytical expressions based on the Fisher matrix approach.

As one can easily expect, the measurement error for $\ddot{f}$ depends strongly on the time baseline of the observation. Therefore, our study will be useful for designing the mission lifetime of LISA or coordinating its collaboration with other detectors such as Taiji [14] and TianQin [15].

This paper is organized as follows. In Sec. II, we briefly summarize the recent long-term orbital analysis for HM Cancri. We also mention some astrophysical implications of the observed results. In Sec. III, applying the Fisher matrix approach to a simplified phase model, we analytically evaluate the estimation errors for phase related parameters such as $\dot{f}$ and $\ddot{f}$. In Sec. IV, we examine the validity of our analytical expressions, by comparison with the full Fisher matrix predictions including all the fitting parameters. In Sec. V, we discuss the observational prospects of measuring $\ddot{f}$ for HM Cancri with LISA. We also apply our analytical expressions to two other verification binaries. In Sec. IV, we discuss issues related to our study. Section VII is a short summary of this paper.

II. LONG-TERM ORBITAL EVOLUTION OF HM CANCRI

A. Observed results

Using x-ray data accumulated in the past $\sim$20 yr, Strohmayer [3] examined the long-term orbital evolution

of HM Cancri. He fitted its phase evolution with the following cubic function:

$$\Phi(t) = 2\pi\left(ft + \frac{\dot{f}t^2}{2!} + \frac{\ddot{f}t^3}{3!}\right) + \varphi \tag{1}$$

with the time origin $t = 0$ at a certain epoch in January 2004. The fitted parameters (after the aforementioned conversions) are

$$f = 0.0062 \text{ Hz}, \tag{2}$$

$$\dot{f} = (7.11 \pm 0.01) \times 10^{-16} \text{ Hz s}^{-1}, \tag{3}$$

$$\ddot{f} = (-1.79 \pm 0.28) \times 10^{-26} \text{ Hz s}^{-2}. \tag{4}$$

Here the error bars represent the 1σ uncertainties.

Munday *et al.* [4] analyzed HM Cancri's optical data with a baseline of ~20 yr and found a good fit to the cubic functional form (1). Their fitted second derivative $\ddot{f}$ is

$$\ddot{f} = (-1.08 \pm 0.42) \times 10^{-26} \text{ Hz s}^{-2}. \tag{5}$$

Note that the error bars in Eqs. (4) and (5) are nearly overlapped. Below, we mainly use Eq. (4) as a reference value of $\ddot{f}$.

B. Astrophysical implications

Before studying the parameter estimation errors with LISA, we briefly discuss some astrophysical implications of the observed long-term orbital evolution of HM Cancri.

As mentioned in the previous subsection, it took ~20 yr to resolve the second frequency derivative $\ddot{f}$ for HM Cancri. In contrast, shortly after the identification of this binary, its chirp rate $\dot{f}$ was measured at a value close to Eq. (3) [16,17]. If the gravitational radiation reaction dominates the observed chirp rate $\dot{f}$, we should have

$$\dot{f} \simeq \dot{f}_{\rm R} = \frac{96\pi^{8/3}G^{5/3}f^{11/3}\mathcal{M}^{5/3}}{5c^5} \tag{6}$$

$$= 7.0 \times 10^{-16}\left(\frac{f}{6.2 \text{ mHz}}\right)^{11/3}\left(\frac{\mathcal{M}}{0.32M_\odot}\right)^{5/3}. \tag{7}$$

Given this relation and the observed rate $\dot{f}$, the chirp mass of HM Cancri was roughly estimated to be $\mathcal{M} \sim 0.3M_\odot$ [3,4]. If this binary is mainly evolved by the gravitational radiation reaction, we also have $\ddot{f} \simeq \ddot{f}_R = 11\dot{f}^2/(3f) \sim 1.5 \times 10^{-28}$ Hz s^{-2} as predicted long before the actual measurement of $\ddot{f}$ [5]. Interestingly, the observed result (4) is totally different from the predicted one $\ddot{f}_{\rm R}$.

Using the Modules for Experiments in Stellar Astrophysics (MESA) code [18], Munday *et al.* [4] compared the observed values $(\dot{f}, \ddot{f})$ with the simulated frequency evolution of many WD binaries. They pointed out that HM Cancri might be shortly ($\sim 10^3$ yr) before the frequency maximum and discovered with the help of a selection effect (see also [3]).

On another front, observations suggest that a significant fraction of close white dwarf binaries might be in triple or higher-order multiple systems [19] (see also [9,20] in the context of LISA observation). In [10] the author argued the possibility that HM Cancri has a tertiary component. For a circular outer orbit with a period P_3 (much longer than the observation period), the tertiary perturbation generates the following shifts to the frequency derivatives (see Refs. [21,22] for similar effects on pulsar timing analysis):

$$\dot{f}_3 = 1.0 \times 10^{-16} F \cos\varphi_3 \left(\frac{f}{6.2 \text{ mHz}}\right)\left(\frac{M_T}{2M_\odot}\right)^{1/3} \times \left(\frac{P_3}{250 \text{ yr}}\right)^{-4/3} \text{Hz s}^{-1}, \tag{8}$$

$$\ddot{f}_3 = -8.0 \times 10^{-26} F \sin\varphi_3 \left(\frac{f}{6.2 \text{ mHz}}\right)\left(\frac{M_T}{2M_\odot}\right)^{1/3} \times \left(\frac{P_3}{250 \text{ yr}}\right)^{-7/3} \text{Hz s}^{-2}. \tag{9}$$

Here M_T is the total mass of the triple system, φ_3 is the outer orbital phase, and $F = m_3 \sin I_3/M_T$ is a projection factor with the tertiary mass m_3 and the outer inclination angle I_3. Therefore, a dark tertiary component (e.g., an old WD with an outer orbital period of ~250 yr) can serve as the main cause for the observed value $\ddot{f}$, with a limited impact on the observed first derivative $\dot{f}$ [see Eqs. (3), (4). (8), and (9)] [10].

As mentioned earlier, during its operation period, LISA is expected to detect $\sim 10^4$ Galactic compact binaries [1]. In particular, it will make a complete Galactic survey for binaries at $f \gtrsim 5$ mHz [1]. Many of the detected binaries might have intensified rates $\ddot{f}$ due to their tertiaries. If this is the case, the probability distribution function of the observed values $\ddot{f}$ would be nearly symmetric around the origin $\ddot{f} = 0$.

III. SIMPLIFIED PHASE MODEL

In this section, applying the Fisher matrix approach to a simplified GW phase model, we analytically estimate the measurement errors for the phase related parameters such as $\dot{f}$ and $\ddot{f}$ (see also [9,23,24]).

A. Basic prescription

Here the GW phase is assumed to be well described by the following Taylor expansion with the coefficients $\{f, \dot{f}, \ddot{f}\}$ defined at the time origin $t = 0$,

$$h(t) = A\cos[\Phi(t)] \tag{10}$$

$$= A\cos\left[2\pi\left(ft + \frac{\dot{f}t^2}{2!} + \frac{\ddot{f}t^3}{3!}\right) + \varphi\right]. \tag{11}$$

We consider a signal analysis in the time interval $t \in [t_1, t_1 + T]$ with the initial time t_1 and the observational duration T. From Parceval's theorem for a nearly monochromatic waveform [25], the signal-to-noise ratio ρ is evaluated as

$$\rho^2 = \frac{2}{S_{\rm n}(f)}\int_{t_1}^{t_1+T} h(t)h(t)dt \tag{12}$$

$$= \frac{A^2 T}{S_{\rm n}(f)} \tag{13}$$

with the measurement noise spectrum $S_{\rm n}(f)$. Note that, as long as the GW signal is nearly monochromatic (i.e., $|\dot{f}|T \ll f$ and $|\ddot{f}|T^2 \ll f$), we can effectively set the true values at $\dot{f} = 0$ and $\ddot{f} = 0$ for evaluating the inner product (12) (also for the Fisher matrix elements below).

Next we apply the Fisher matrix approach to the phase related parameters $\boldsymbol{\theta} = \{\varphi, f, \dot{f}, \ddot{f}\}$ with the waveform model (11). The amplitude parameter A has no correlation with the target parameters $\boldsymbol{\theta}$ and can be dropped from our fitting parameters in this section.

We can formally express the Fisher matrix elements as

$$F_{\theta_i\theta_j} = \frac{2}{S_{\rm n}(f)}\int_{t_1}^{t_1+T} \partial_{\theta_i}h(t)\partial_{\theta_j}h(t)dt. \tag{14}$$

Using Eq. (13), we can eliminate the overall factor $A/S_{\rm n}(f)$ and then present the matrix elements $F_{\theta_i\theta_j}$ in terms of ρ, t_1, and T. For example, we have

$$F_{ff} = 4\pi^2\rho^2\left(\frac{3t_1^2 + 3t_1T + T^2}{3}\right). \tag{15}$$

After taking the inverse of the matrix F, we can evaluate the covariance matrix of the parameter estimation error $\delta\theta_i$ as

$$\langle\delta\theta_i\delta\theta_j\rangle = (F^{-1})_{\theta_i\theta_j}. \tag{16}$$

Below, for notational simplicity, we put the rms errors by

$$\Delta\theta_i \equiv \langle\delta\theta_i\delta\theta_i\rangle^{1/2} \tag{17}$$

and denote the correlation factor by

$$C_{\theta_i\theta_j} \equiv \frac{\langle\delta\theta_i\delta\theta_j\rangle}{\langle\delta\theta_i\delta\theta_i\rangle^{1/2}\langle\delta\theta_j\delta\theta_j\rangle^{1/2}} \tag{18}$$

with the Cauchy-Schwartz inequality $|C_{\theta_i\theta_j}| \le 1$.

B. Expansion at the initial epoch

Following the outline in the previous subsection, we now evaluate the Fisher matrix F for the observational time domain $t \in [0, T]$ with the initial epoch at $t_1 = 0$. This means that the GW phase is Taylor expanded as in Eq. (11) at the initial epoch $t = t_1 = 0$. For the four basic parameters $\boldsymbol{\theta} = \{\varphi, f, \dot{f}, \ddot{f}\}$, we can easily obtain the rms errors as

$$\Delta\varphi = \frac{4}{\rho},\quad \Delta f = \frac{10\sqrt{3}}{\pi\rho T},\quad \Delta\dot{f} = \frac{36\sqrt{5}}{\pi\rho T^2},\quad \Delta\ddot{f} = \frac{60\sqrt{7}}{\pi\rho T^3}. \tag{19}$$

We provide some examples of the correlation coefficients

$$C_{\dot{f}\ddot{f}} = -\frac{\sqrt{35}}{6} \simeq -0.986,$$
$$C_{f\ddot{f}} = -\frac{\sqrt{21}}{5} \simeq -0.917. \tag{20}$$

Robson *et al.* [9] obtained essentially the same results as Eq. (19), while their definitions for the evolutionary parameters $(\dot{f}, \ddot{f})$ are slightly different from ours (see their appendix).

Next, for a comparison purpose, we drop the cubic term $\propto\ddot{f}t^3$ in Eq. (11) as

$$h_{\rm tr}(t) = A\cos\left[2\pi\left(ft + \frac{\dot{f}t^2}{2!}\right) + \varphi\right]. \tag{21}$$

Using this truncated waveform model studied in [23], we can derive the analytical results for the smaller set $\boldsymbol{\theta} = \{\varphi, f, \dot{f}\}$ as follows:

$$\Delta\varphi = \frac{3}{\rho},\qquad \Delta f = \frac{4\sqrt{3}}{\pi\rho T},\qquad \Delta\dot{f} = \frac{6\sqrt{5}}{\pi\rho T^2}, \tag{22}$$

which are identical to the corresponding expressions in [23]. Compared with Eq. (19), we can see a large reduction of the error $\Delta\dot{f}$.

C. Expansion at the midpoint

Next we evaluate the Fisher matrix prediction for the observational time domain $t \in [-T/2, T/2]$, setting the initial epoch at $t_1 = -T/2$. In this choice, the GW phase is Taylor expanded as Eq. (11) at the midpoint ($t = 0$) of the observational period. The estimation errors for the parameters $\{\varphi_0, \dot{f}\}$ and those for $\{f, \ddot{f}\}$ are statistically uncorrelated, and the matrices F and F^{-1} are block diagonal.

This is because we have the symmetric cancellations at integrating odd functions such as

$$F_{\ddot{f}\dot{f}} \propto \int_{-T/2}^{T/2} t^{2+3} dt = 0. \tag{23}$$

For the fitting parameters $\boldsymbol{\theta} = \{\varphi, f, \dot{f}, \ddot{f}\}$, the rms errors are estimated to be

$$\Delta\varphi = \frac{3}{2\rho}, \qquad \Delta f = \frac{5\sqrt{3}}{2\pi\rho T},$$
$$\Delta\dot{f} = \frac{6\sqrt{5}}{\pi\rho T^2}, \qquad \Delta\ddot{f} = \frac{60\sqrt{7}}{\pi\rho T^3} \tag{24}$$

with some examples for the correlation coefficients as

$$C_{\dot{f}\ddot{f}} = 0, \qquad C_{f\ddot{f}} = -\frac{\sqrt{21}}{5}. \tag{25}$$

As in the case of Eq. (22), the magnitude $\Delta\dot{f}$ is largely reduced from Eq. (19). In contrast, the results for $\Delta\ddot{f}$ are the same in Eqs. (19) and (24). We can understand this from the following argument. Given the difference between the time origins ($t_1 = 0$ or $-T/2$), we can relate the parameters $\{\varphi, f, \dot{f}, \ddot{f}\}$ in this subsection with those $\{\varphi_{\rm o}, f_{\rm o}, \dot{f}_{\rm o}, \ddot{f}_{\rm o}\}$ (temporarily attaching the subscript "o") in the previous subsection. For example, we have

$$\dot{f} = \dot{f}_{\rm o} + \ddot{f}_{\rm o} T/2, \qquad \ddot{f} = \ddot{f}_{\rm o}, \tag{26}$$

resulting in $\Delta\ddot{f} = \Delta\ddot{f}_{\rm o}$ for optimal signal analyses.

We again examine the truncated model (21) and obtain the associated measurement errors under the midpoint expansion as

$$\Delta\phi = \frac{3}{2\rho}, \qquad \Delta f = \frac{\sqrt{3}}{\pi\rho T}, \qquad \Delta\dot{f} = \frac{6\sqrt{5}}{\pi\rho T^2}. \tag{27}$$

Because of the block diagonalization, the magnitudes $\Delta\phi$ and $\Delta\dot{f}$ are the same as Eq. (24). Furthermore, due to the reason similar to Eq. (26), we have the same expression $\Delta\dot{f}$ in Eqs. (22) and (27).

IV. COMPARISON WITH FULL FISHER MATRIX ANALYSIS

Our simplified analytical models in the previous section lack the amplitude and Doppler phase modulations, which are induced by the annual motion of LISA [25]. In this subsection, we examine the validity of our simple analytical results (19) and (24), by comparing them with the full Fisher matrix results evaluated numerically.

For the full Fisher matrix estimation, we deal with the following nine fitting parameters $\{A, \varphi, f, \dot{f}, \ddot{f}, \theta_S, \phi_S, \theta_L, \phi_L\}$, extending the formulation in [25]. The pairwise angular parameters $\{\theta_S, \phi_S\}$ and $\{\theta_L, \phi_L\}$, respectively, specify the source direction and orientation in the ecliptic coordinate.

Here we comment on an earlier study related to this section. Takahashi and Seto [26] briefly compared the analytical results (22) [for the truncated model (21)] with the corresponding numerical results. The latter were obtained from the full 8×8 Fisher matrices (without the parameter $\ddot{f}$). They found that, for $T \gtrsim 2$ yr, the analytical and numerical results agree quite well. This is because, for $T \gtrsim 2$ yr, the intrinsic frequency evolution in Eq. (21) is well separable from the annual periodic phase shift induced by LISA's motion. Even adding the cubic term as Eq. (11), we can expect a similar trend.

For numerically evaluating the 9×9 Fisher matrix, we randomly generated 20 realizations for the combinations $\{\theta_S, \phi_S, \theta_L, \phi_L\}$, assuming that the direction and orientation vectors are isotropically distributed. At $f = 1$ mHz and 10 mHz, we numerically evaluated the estimation errors $(\Delta\dot{f}_{\rm full}, \Delta\ddot{f}_{\rm full})$ and compared them with the analytical ones $(\Delta\dot{f}_{\rm ana}, \Delta\ddot{f}_{\rm ana})$ given in the previous section. Only in this section, we use the subscripts "full" and "ana," respectively, for the full Fisher matrix estimations and the analytical ones.

In Fig. 1, for $T = 1, 2, 4, 6$, and 8 yr, we present the ratio $\Delta\ddot{f}_{\rm full}/\Delta\ddot{f}_{\rm ana}$ for the second derivative $\ddot{f}$ with a small horizontal offset for the midpoint expansion. As shown in Eqs. (19) and (24), the analytical expression $\Delta\ddot{f}_{\rm ana} = 60\sqrt{7}/(\pi\rho T^3)$ is identical in the two expansion methods. Consistent with the argument around Eq. (26), Fig. 1 clearly shows that the numerical results $\Delta\ddot{f}_{\rm full}$ are also the same for the two expansion methods (except for tiny numerical errors).

At $T \gtrsim 2$ yr, the mismatches between the two estimations $\Delta\ddot{f}_{\rm full}$ and $\Delta\ddot{f}_{\rm ana}$ are less than 50%. In reality, a long-term signal integration is essential for measuring the second derivative $\ddot{f}$, and the mismatches are even less than ~5% at $T \gtrsim 8$ yr.

In contrast, for $T = 1$ yr, the analytical estimation $\Delta\ddot{f}_{\rm ana}$ underestimates the full estimation $\Delta\ddot{f}_{\rm full}$, generally showing larger mismatches at $f = 10$ mHz. This frequency dependence can be understood from the relative importance of the amplitude modulation for estimating the source direction. With a LISA-like detector, we can determine the source direction from the Doppler phase modulation and the amplitude modulation, both induced by the annual motion of the detector [25]. If the signal-to-noise ratio is fixed, the former is proportional to the frequency but the latter is independent of it. Therefore, at the lower frequency regime, the amplitude modulation can work more efficiently to suppress the interference between the Doppler phase modulation and the intrinsic phase evolution.

In their appendix, Robson *et al.* [9] derived an analytical expression [essentially corresponding to $\Delta\ddot{f}_{\rm ana}$ in Eq. (19)].

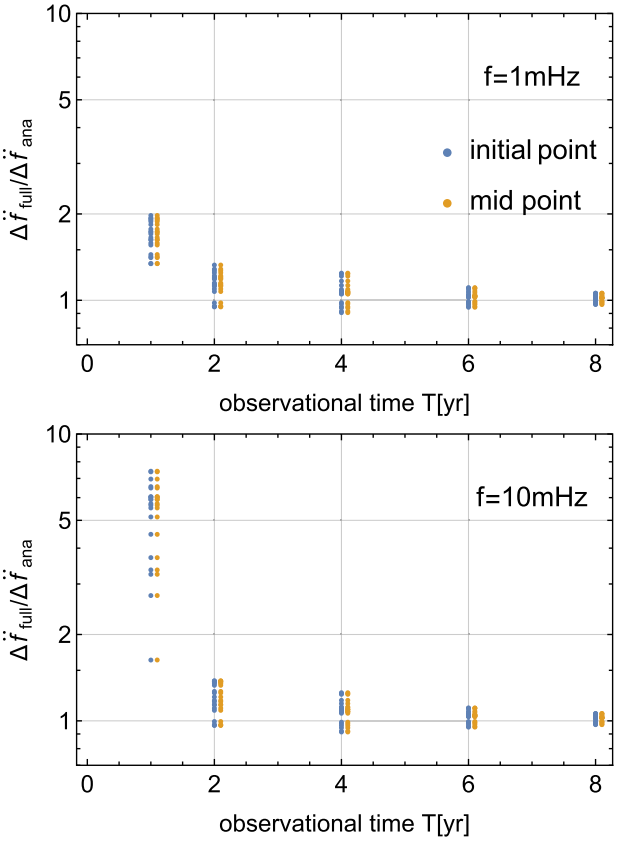

FIG. 1. Ratios $\Delta\ddot{f}_{\rm full}/\Delta\ddot{f}_{\rm ana}$ between the full Fisher matrix predictions $\Delta\ddot{f}_{\rm full}$ and those with the analytical estimation $\Delta\ddot{f}_{\rm ana} = 60\sqrt{7}/(\pi\rho T^3)$ given in Eqs. (19) and (24). We show the results for 20 randomly sampled binaries with the initial and midpoint expansions. The upper panel is for $f = 1$ mHz and the lower one for 10 mHz.

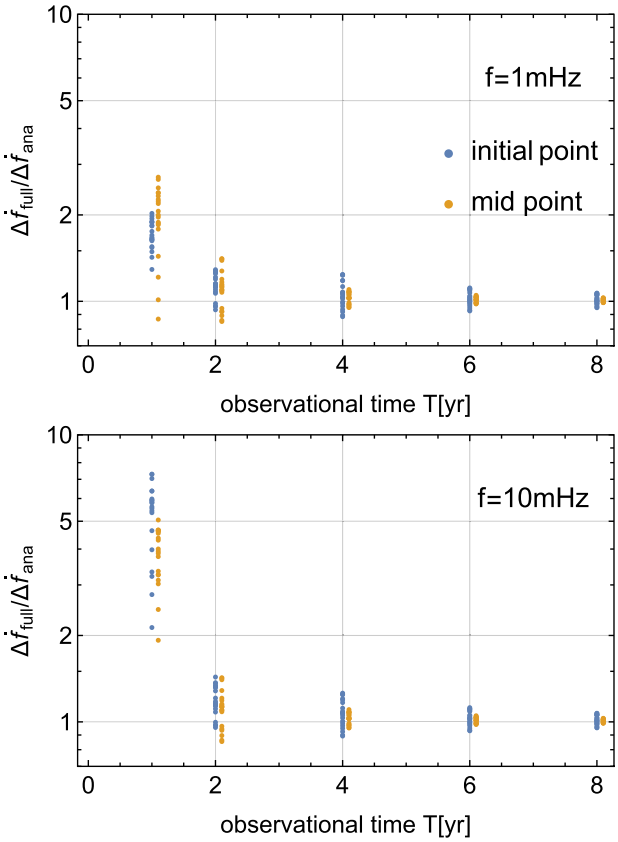

FIG. 2. Similar to Fig. 1 but for the ratio $\Delta\dot{f}_{\rm full}/\Delta\dot{f}_{\rm ana}$. Note that, between the two expansion methods, the denominator $\Delta\dot{f}_{\rm ana}$ is different by a factor of 6, as presented in Eqs. (19) and (24).

They also compared it with a full Fisher matrix prediction. For a certain set of the geometric parameters $\{\theta_S, \phi_S, \theta_L, \phi_L\}$ at $f = 5$ mHz, they reported a mismatch of $\Delta\ddot{f}_{\rm full}/\Delta\ddot{f}_{\rm ana} \sim 6$. While they did not explicitly present the applied integration period T, our Fig. 1 indicates that their choice is likely to be $T \sim 1$ yr.

In Fig. 2, we show the ratio $\Delta\dot{f}_{\rm full}/\Delta\dot{f}_{\rm ana}$ for the first derivative $\dot{f}$. Now, the analytical results $\Delta\dot{f}_{\rm ana}$ are different between the two expansion methods [compare Eqs. (19) and (24)]. In any case, we can again confirm that, at $T \gtrsim 2$ yr, the analytical results $\Delta\dot{f}_{\rm ana}$ well reproduce the numerical ones $\Delta\dot{f}_{\rm full}$.

The ratios in Figs. 1 and 2 are slightly less than unity for some binary samples, even though the number of fitting parameters are larger for the numerator. This is actually not surprising, given the time dependence of the signal accumulation. In contrast to the flat weighting for the analytic model as in Eq. (12), the full Fisher matrix evaluation has the annual amplitude modulation. Considering the advantage of a longer baseline at estimating the variation rates $\dot{f}$ and $\ddot{f}$, the errors $(\Delta\dot{f}_{\rm full}, \Delta\ddot{f}_{\rm full})$ can be smaller for a binary whose signal strength is relatively large around the initial and the final epochs.

At $T \gtrsim 2$ yr, the simple analytic expressions $(\Delta\dot{f}_{\rm ana}, \Delta\ddot{f}_{\rm ana})$ work well, even if we remove the source direction angles $\{\theta_S, \phi_S\}$ from our fitting parameters (e.g., after identifying the EM counterpart). We can easily understand this from the weak correlation between the intrinsic phase parameters and the direction angles at $T \gtrsim 2$ yr.

We should also note that the full Fisher matrix predictions still have some deviations from more elaborate evaluations such as Markov chain Monte Carlo simulations [9] (see also [27]). Nevertheless, the Fisher matrix predictions (in particular, our analytical expressions) will be convenient guides for discussing parameter estimation errors.

V. OBSERVATIONAL PROSPECTS WITH LISA

Now, for existing binaries such as HM Cancri, we discuss the prospects of measuring $\dot{f}$ and $\ddot{f}$ with LISA. We apply our analytical expressions derived in Sec. III.

A. HM Cancri

The distance d to HM Cancri has large uncertainties [3,4]. Below, we use the reference value $d = 5$ kpc,

following [2]. Then, including geometrical parameters, LISA will detect its quadrupole GW at the signal-to-noise ratio of

$$\rho = 210\left(\frac{T}{4\ \mathrm{yr}}\right)^{1/2}\left(\frac{d}{5\ \mathrm{kpc}}\right)^{-1}\left(\frac{\mathcal{M}}{0.33M_\odot}\right)^{5/3}. \quad (28)$$

Now we discuss the parameter estimation errors for the frequency derivatives $\dot{f}$ and $\ddot{f}$. Here we solely use the expressions in Eq. (24) for the midpoint expansion. Note that, as mentioned earlier, for the first derivative, the expression $\Delta\dot{f} = 6\sqrt{5}/(\pi\rho T^2)$ in Eq. (24) is identical to those in Eqs. (22) and (27), which are given for the truncated model (21). Therefore, we can apply this expression under various situations.

From Eqs. (24) and (28), at $T \gtrsim 2$ yr, we can expect the estimation errors for HM Cancri as follows:

$$\Delta\dot{f} = 1.3\times10^{-18}\left(\frac{\rho}{210}\right)^{-1}\left(\frac{T}{4\ \mathrm{yr}}\right)^{-2}\ \mathrm{Hz\,s^{-1}}, \quad (29)$$

$$\Delta\ddot{f} = 1.2\times10^{-25}\left(\frac{\rho}{210}\right)^{-1}\left(\frac{T}{4\ \mathrm{yr}}\right)^{-3}\ \mathrm{Hz\,s^{-2}}. \quad (30)$$

Now let us compare these expressions with the actual observational results (3) and (4). The nominal operation period of LISA is planned to be $T \sim 4$ yr with a possible extension to $\sim$10 yr. For $T \sim 4$ yr, we can realize a good resolution $\Delta\dot{f}$ comparable to the error bar in Eq. (3).

Meanwhile, for $T \sim 4$ yr, we can only set a loose bound to the observed value $\ddot{f}$ (i.e., $\Delta\ddot{f} > |\ddot{f}|$). However, given the strong scaling relation $\Delta\ddot{f} \propto \rho^{-1}T^{-3} \propto T^{-7/2}$ (valid for $T \gtrsim 2$ yr), we should not be too pessimistic. Indeed, compared with $T = 4$ yr, the resolution $\Delta\ddot{f}$ will be improved by a factor of $\sim$25 and $\sim$100, respectively, for $T = 10$ and 15 yr. Therefore, with these extended time baselines, we can reach $\Delta\ddot{f} = 0.72\times10^{-26}\ \mathrm{Hz\,s^{-2}}$ and $0.18\times10^{-26}\ \mathrm{Hz\,s^{-2}}$, corresponding to 40% and 10% of the reference value (4).

Note that LISA also allows us to estimate the intrinsic GW amplitude $\mathcal{A} \simeq \mathcal{M}^{5/3}/d$ with the typical accuracy of $\Delta\mathcal{A}/\mathcal{A} \sim 0.2(\rho/10)^{-1}$ [26]. If the observed chirp rate $\dot{f}$ is dominated by the radiation reaction as in Eq. (6), we can estimate the chirp mass $\mathcal{M}$ and thereby the source distance d. However, HM Cancri is an interacting binary, and we should be careful to apply Eq. (6) to this system. In any case, using certain priors to its chirp mass distribution, we will be able to constrain its distance d much better than the current estimation.

B. V407 Vul and SDSS J0651

Here we apply Eqs. (29) and (30) to two other well-known verification binaries (see Ref. [2] for their basic parameters).

V407 Vul is likely to be an interacting WD binary at the estimated distance of $d = 1.8$ kpc. Its GW frequency is $f = 3.5$ mHz with the observed chirp rate $\dot{f} = 2.0\times10^{-17}\ \mathrm{Hz\,s^{-1}}$. After a 4 yr integration, LISA is expected to observe its GW at $\rho = 170$. From Eq. (29), at $T = 4$ yr, we will have the resolution $\dot{f}/\Delta\dot{f} = 12$. If we can operate LISA for 10 yr, the tertiary perturbation $\ddot{f}_3$ in Eq. (9) can be resolved at the 3σ level (i.e., $|\ddot{f}_3|/\Delta\ddot{f} > 3$) for an outer orbital period of $P_3 < 280$ yr. Here we put $F = 0.5$, $M_T = 2.0M_\odot$, and $\sin\varphi_3 = 1$ in Eq. (9). For $T = 15$ yr, we obtain $P_3 < 500$ yr.

SDSS J0651 is a detached WD binary at $d = 0.93$ kpc with $f = 2.6$ mHz and $\dot{f} = 3.3\times10^{-17}\ \mathrm{Hz\,s^{-1}}$. For $T = 4$ yr, the expected signal-to-noise ratio is $\rho = 90$ with the resolution $\dot{f}/\Delta\dot{f} = 11$. For $T = 10$ yr, a tertiary perturbation $\ddot{f}_3$ can be resolved at the 3σ level for $P_3 < 180$ yr. Since this system is a detached binary, its distance d will be estimated relatively well, only from GW observation.

VI. DISCUSSIONS

A. Other detectors

So far, we have focused on observation with LISA. Around 4–20 mHz, the Chinese proposal Taiji is planned to have $\sim$1.5 better sensitivity $\sqrt{S_n(f)}$ than LISA [14]. Moreover, HM Cancri is a very special target for another Chinese project TianQin [15]. Indeed, the orbital configuration of TianQin is designed to optimally detect this binary [15]. By combining these missions with LISA, we might effectively realize a long time baseline of $T \gtrsim 15$ yr and finely measure $\ddot{f}$ for many binaries. The Japaneses projects B-DECIGO and DECIGO are planned to explore the 0.1 Hz band [28,29] and can also contribute to this observational campaign.

B. Relation to EM observations

In the previous section, we made a case study for HM Cancri, as a representative target for LISA. Now let us suppose that LISA actually observes HM Cancri from 2035 to 2050 ($T \sim 15$ yr). At the time of 2050, its EM data have the total duration of $\sim$50 yr (from $\sim$2000) and the resultant resolution $\Delta\ddot{f}$ would be much better than that from the GW observation. Nevertheless, the direct comparison between the EM and the GW results will be meaningful for HM Cancri. In particular, GW emission in itself is robustly related to the binary orbital motion with basically no need for internal dissipation models.

VII. SUMMARY

Recently, for HM Cancri, Strohmayer [3] and Munday *et al.* [4] measured the second frequency derivative $\ddot{f} \sim -10^{-26}\ \mathrm{Hz\,s^{-2}}$, using x-ray and optical data accumulated in the past $\sim$20 yr. Their results will be good

reference values for numerous Galactic binaries to be detected by LISA.

In this paper, based on a simplified phase model, we present analytical expressions for the estimation errors of the phase related parameters. Our analytical expressions work well for an observational period $T \gtrsim 2$ yr. For HM Cancri, LISA is unlikely to realize a sufficient resolution $\Delta\ddot{f}$ in its nominal operation period 4 yr. However, because of the strong scaling relation $\Delta\ddot{f} \propto T^{-7/2}$, we can make a much better resolution by extending the operation period of LISA or combining it with other detectors in a sequential order.

ACKNOWLEDGMENTS

The author thanks N. Cornish for correspondence. This work is supported by JSPS Kakenhi Grant-in-Aid for Scientific Research (No. 19K03870 and No. 23K03385).

[1] P. Amaro-Seoane *et al.* (LISA Collaboration), Living Rev. Relativity **26**, 2 (2023).
[2] T. Kupfer, V. Korol, S. Shah, G. Nelemans, T. R. Marsh, G. Ramsay, P. J. Groot, D T H Steeghs, and E M Rossi, Mon. Not. R. Astron. Soc. **480**, 302 (2018).
[3] T. E. Strohmayer, Astrophys. J. Lett. **912**, L8 (2021).
[4] J. Munday, T. R. Marsh, M. Hollands, I. Pelisoli, D. Steeghs, P. Hakala, E. Breedt, A. Brown, V. S. Dhillon, M. J. Dyer *et al.*, Mon. Not. R. Astron. Soc. **518**, 5123 (2022).
[5] C. J. Deloye and R. E. Taam, Astrophys. J. Lett. **649**, L99 (2006).
[6] F. D'Antona, P. Ventura, L. Burderi, and A. Teodorescu, Astrophys. J. **653**, 1429 (2006).
[7] D. L. Kaplan, L. Bildsten, and J. D. R. Steinfadt, Astrophys. J. **758**, 64 (2012).
[8] S. Biscoveanu, K. Kremer, and E. Thrane, Astrophys. J. **949**, 95 (2023).
[9] T. Robson, N. J. Cornish, N. Tamanini, and S. Toonen, Phys. Rev. D **98**, 064012 (2018).
[10] N. Seto, arXiv:2307.09739.
[11] G. Nelemans, L. R. Yungelson, and S. F. Portegies Zwart, Mon. Not. R. Astron. Soc. **349**, 181 (2004).
[12] A. Lamberts, S. Blunt, T. B. Littenberg, S. Garrison-Kimmel, T. Kupfer, and R. E. Sanderson, Mon. Not. R. Astron. Soc. **490**, 5888 (2019).
[13] N. Seto, Phys. Rev. Lett. **128**, 041101 (2022).
[14] W. H. Ruan, Z. K. Guo, R. G. Cai, and Y. Z. Zhang, Int. J. Mod. Phys. A **35**, 2050075 (2020).
[15] J. Luo *et al.* (TianQin Collaboration), Classical Quantum Gravity **33**, 035010 (2016).
[16] G. L. Israel, S. Covino, S. Dall'Osso, D. Fugazza *et al.*, Mem. S. A. It. Suppl. **5**, 148 (2004).
[17] T. E. Strohmayer, Astrophys. J. **627**, 920 (2005).
[18] B. Paxton, R. Smolec, J. Schwab, A. Gautschy, L. Bildsten, M. Cantiello, A. Dotter *et al.*, Astrophys. J. Suppl. Ser. **243**, 10 (2019).
[19] S. Toonen, M. Hollands, B. T. Gänsicke, and T. Boekholt, Astron. Astrophys. **602**, A16 (2017).
[20] Z. Xuan, P. Peng, and X. Chen, Mon. Not. R. Astron. Soc. **502**, 4199 (2021).
[21] C. G. Bassa, G. H. Janssen, B. W. Stappers, T. M. Tauris, T. Wevers, P. G. Jonker, L. Lentati, J. P. W. Verbiest, G. Desvignes, E. Graikou *et al.*, Mon. Not. R. Astron. Soc. **460**, 2207 (2016).
[22] D. L. Kaplan, T. Kupfer, D. J. Nice, A. Irrgang, U. Heber, Z. Arzoumanian, E. Beklen, K. Crowter, M. E. DeCesar, P. B. Demorest *et al.*, Astrophys. J. **826**, 86 (2016).
[23] N. Seto, Mon. Not. R. Astron. Soc. **333**, 469 (2002).
[24] S. Shah and G. Nelemans, Astrophys. J. **791**, 76 (2014).
[25] C. Cutler, Phys. Rev. D **57**, 7089 (1998).
[26] R. Takahashi and N. Seto, Astrophys. J. **575**, 1030 (2002).
[27] M. Vallisneri, Phys. Rev. D **77**, 042001 (2008).
[28] N. Seto, S. Kawamura, and T. Nakamura, Phys. Rev. Lett. **87**, 221103 (2001).
[29] S. Kawamura *et al.*, Prog. Theor. Exp. Phys. **2021**, 05A105 (2021).